EIGENVALUES FOR THE RF CAVITIES IN THE ING LINEAR ACCELERATOR

A Thesis

Presented To

The Faculty of Graduate Studies And Research

The University of Manitoba

In Partial Fulfillment

of the Requirements for the Degree

Master of Science in Electrical Engineering

by

Prakash Bhartia

September 1968

ABSTRACT

To accelerate protons in an Alvarez type linear accelerator or electrons in velocity modulated tubes, the cavity must be excited in the dominant TM_{olo} mode. For proper understanding of beam dynamics and for purposes of design, the r.f. fields must be computed accurately for any specified dimensions of the drift space. In this thesis the exact numerical solution for the fields in a drift tube loaded linear accelerator cavity with a beam guiding hole is presented. The eigenvalues, field distributions, transit time factor and the shunt impedance are formulated everywhere by boundary value techniques in the same manner as proposed by Bolle and Gluckstern in the absence of the beam guiding hole. The numerical results are obtained with the aid of a digital computer and are verified by excellent agreement with an experimental method based on perturbation techniques.

ACKNOWLEDGMENTS

The author expresses his sincere appreciation to Professor M.A.K. Hamid who suggested the problem and took an active interest in the work throughout.

Acknowledgement is due to Professor E. Bridges who supervised the experimental portion and made the results available for publication. Thanks are due to friends and colleagues for their comments and discussions and to Miss S. Yamaguchi for the expertly typed manuscript.

The financial assistance of the Atomic Energy of Canada Limited under Contract No. 01-323-35 is also acknowledged.

TO MY PARENTS

WITH DEEP GRATITUDE AND AFFECTION

TABLE OF CONTENTS

LIST OF FIGURES

CHAPTER I

INTRODUCTION

Two types of cavities, both represented schematically by figure 1.1, operating in one of the o-2π modes, with a field configuration similar to that of the TM_{01n} mode in a cylindrical cavity are used in Linear Accelerators (linacs). In addition, these structures have a very important role in velocity modulated tubes. Practical linac cavities differ from this only slightly due to the stems supporting the drift tube and the complexity of the r.f. feed system. For proper understanding of linac behaviour under various perturbing factors and interactions, and for accurate calculations of beam loading effects and energy gain of the particles, it is very essential to have an accurate knowledge of the field distribution in the accelerating cavities.

Closed form solution for the r.f. fields in accelerating cavities with structural perturbations and interactions with the loading beam have been difficult to obtain in the past, and instead, a functional representation on basis of experimental data is usually made [1-4] . Linac behaviour is then calculated and explained using these expressions. Another approach to the problem has been from a circuit point of view, where the cavity is represented in terms of an equivalent circuit which is used to solve for the resonant frequency, dispersion relations and beam loading effects. A number of authors have formulated the solution using the normal mode analysis together with indirect or experimental methods to evaluate the fields[1, 3, 7-9] , but no significant attempt to solve the boundary value problem has been made. Numerical techniques have also been used

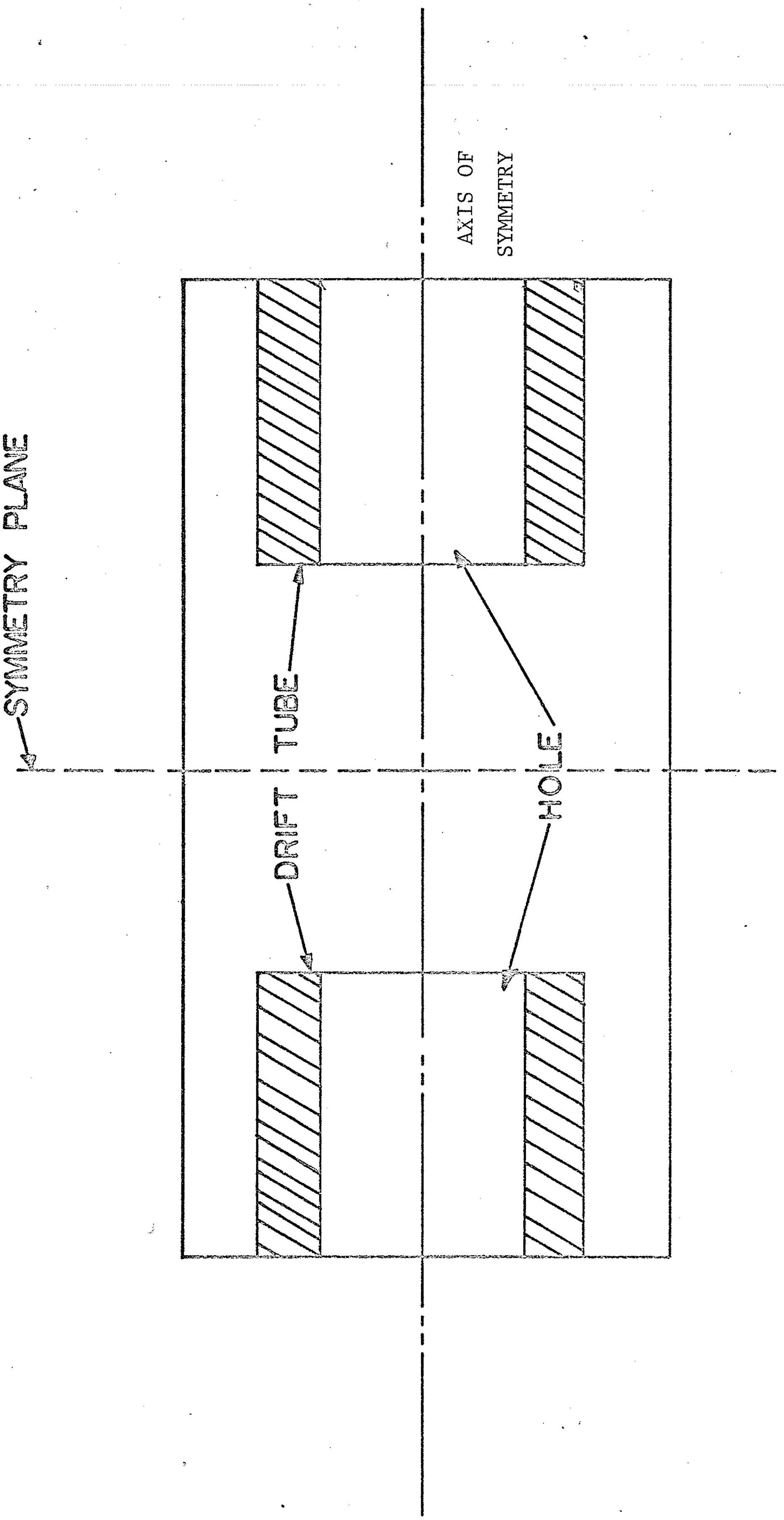

FIG. 1.1 THE ALAREZ CAVITY

to analyse the fields [10] and this approach led to the elaborate LALA (Los Alamos Linear Accelerator) program which Hoyt [11] used to optimize the design of the cavity.

In this thesis, the exact boundary value formulation is presented for the drift tube loaded cylindrical cavity,taking into consideration the beam guiding hole. The method used is that proposed by Hahn [12] and extended by Bolle [13] to deal with the centerally loaded cavity.

The basis of the method lies in subdividing the space,for which the fields are required,into suitable regions. The wave equation is solved independently in each region using a suitable coordinate system. The boundary conditions on the mettalic surfaces are imposed and the fields matched at the interface of adjacent regions resulting in an infinite number of linear simultaneous equations. On elimination of the unknown constants,a single equation results whose solution leads to the desired eigenvalues and field distribution. Further,expressions are developed for the quality factor of the cavity on the basis of an exact derivation for the losses and the energy stored in the system.

In the second part of the thesis,Gluckstern's work [14] is extended using the results mentioned above, to obtain expressions for the transit time factor and shunt impedance, considering the effect of the beam guiding hole which has hitherto not been considered.

Curves for the variation of the eigenvalue with the order of the determinant, and for the axial field versus position, are presented and compared with the experimental results.For the test cavity the calculated and measured values are in agreement to within experimental error.

CHAPTER II

FIELD DISTRIBUTION IN LINAC CAVITIES

At very high frequencies, circuit approximations for resonators are practically invalid, and an exact or rigorous method of calculation is a necessity for direct use in design work or for justifying new approximations to simplify design formulae. A field solution which satisfies the boundary conditions everywhere in the cavity is our objective; and the method used in this chapter meets these requirements in obtaining a solution for the fields in an Alvarez cavity.

2.1 Modes in Linac Cavities

The operating mode of a linac is defined as the shift in the r.f. phase between adjacent cells. The structure can be designed to operate in any mode between 'o' and 'π'. For low proton energies, below 200 Mev, the Alvarez structure is normally operated in the 'o' or '2π' mode as it is called. Here the particles take an entire cycle to pass through the cavity; several cavities are used and no dividing walls are required between adjacent cavities and operation is usually around 200 MHz. For higher energies the 'π'-mode structure is used. Here the average velocity of the particles is such, that they traverse the cell length in ½ a cycle of the r.f. power, so that the phase of adjacent cells must differ by 180°. Since the fields in adjacent cavities are in opposite directions, separation walls are necessary.

Both the above discussed structures can contain drift tubes to concentrate the electric field near the axis of the cavity and hence increase its efficiency in the acceleration of the particles. In the '2π' mode structure, the particles are in the drift tube hole when the electric field is directed to produce deceleration, and hence are shielded from the fields. In the 'π' mode structure, no particles are in the cavity when decelerating fields are present.

2.2 Fields in The Alvarez Structure

In this section expressions are developed for the fields existing in all regions of an Alvarez Structure. This work is an extension of Bolles' [13] solution for the simple drift tube loaded cavity and takes into account the beam guiding bore. The relatively simple technique of field matching is employed to obtain a solution of the fields in the cavity. The cavity space is divided into regions and the axial field is expressed in each region by solving the wave equation in that region, using an appropriate coordinate system which best suits the geometry under consideration. Boundary conditions are applied to obtain the complete solution and the fields at the interface of adjacent regions are matched for continuity. This results in an infinite number of equations which, on elimination of the unknown constants,result in a single equation. The secular determinant of this equation, in terms of the propogation constant, is solved for the particular geometry under consideration.

Once the fields are known, the transit time factor, shunt impedance and other paramaters of importance,in conjunction with the study of linacs, may be accurately evaluated.

2.3 Formulation of The Problem

Consider figure 2.3.1 which shows a drift-tube loaded circular cylindrical cavity with a beam guiding hole. Since the structure has complete symmetry about the axes AA' and BB', it is only necessary to consider a quarter of the structure as shown in figure 2.3.2.

2.3.1 Solution of The Wave Equation

The space is divided into three regions with o as the origin of the cylindrical coordinates. These regions are as follows:

$$
\begin{aligned}
&\text{Region I} \ldots\ldots\ldots \quad o \le z \le s \quad ; \quad o \le r \le c \\
&\text{Region II} \ldots\ldots\ldots \quad s \le z \le L \quad ; \quad b \le r \le c \qquad\qquad (2.3.1) \\
&\text{Region III} \ldots\ldots \quad s \le z \le L \quad ; \quad o \le r \le a
\end{aligned}
$$

The walls of the cavity are assumed perfectly conducting and the interior space is filled with an ideal dielectric. The wave equation in the absence of the beam may be written as

$$(\nabla^2 + k^2)\, E_z = 0 \qquad (2.3.2)$$

where the field E_z is to be expressed in terms of the TM_{oij} modes which are of particular interest in linac structures. Here k is the wave propogation constant. Equation (2.3.2) applies to all three regions, and, since the structure is circularly symmetrical about the z axis, no 'θ' variation is obtained in the solution for the fields.

The solutions for the electric field E_z in the various regions are expressed as follows:

Region I :

$$E_{zI} = \sum_{m=1}^{\infty} A_m J_o(k_m r) \cos(\alpha_m z) \qquad (2.3.3)$$

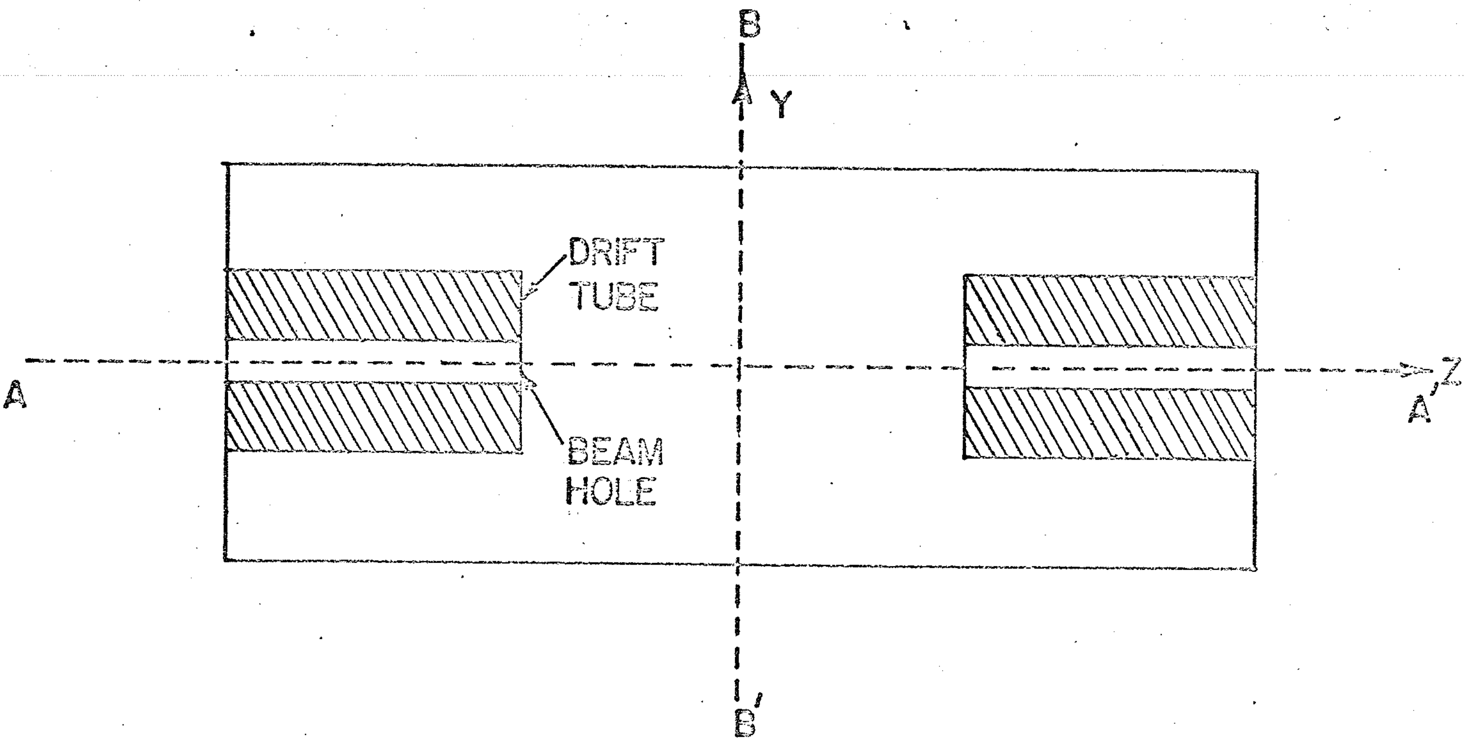

FIG. 2.3.1 CROSS SECTION OF AN ALVAREZ CAVITY

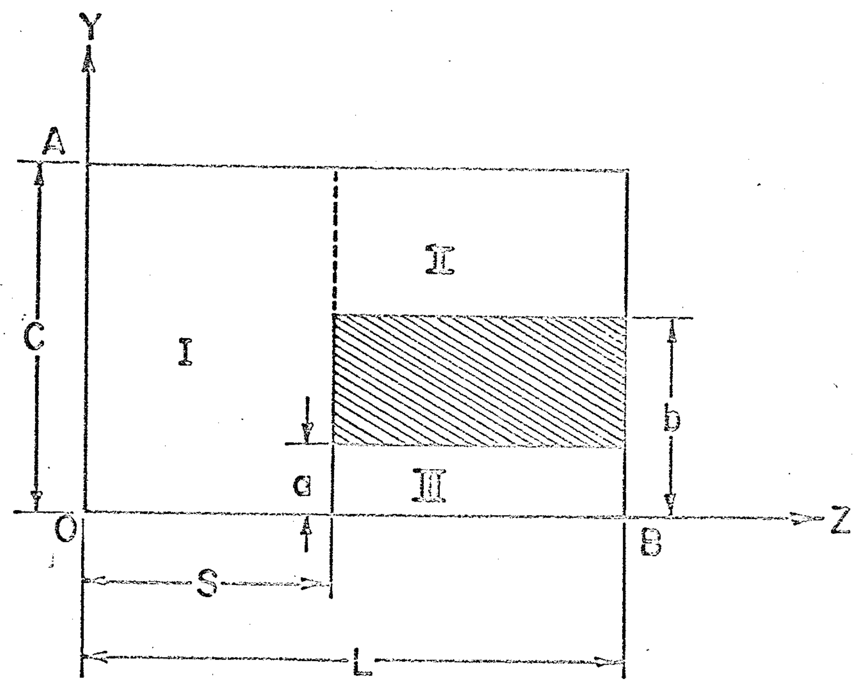

FIG.2.3.2 CAVITY SECTION USED IN THE ANALYSIS

Region II :

$$E_{zII} = \sum_{n=1}^{\infty} B_n Z_n(k_n r) \{ \cos(\beta_n z) + C_n \sin(\beta_n z) \} \tag{2.3.4}$$

Region III : $$E_{zIII} = \sum_{p=1}^{\infty} D_p J_p(k_p r) \{ \cos(\gamma_p z) + F_p \sin(\gamma_p z) \} \tag{2.3.5}$$

where

$$k_m^2 + \alpha_m^2 = k_n^2 + \beta_n^2 = k_p^2 + \gamma_p^2 = k^2 \tag{2.3.6}$$

$$Z_n(k_n r) = J_n(k_n r) + R_n N_n(k_n r) \tag{2.3.7}$$

and where R_n is a constant, J_n and N_n are the Bessel and Neumann functions, respectively, k is the free space propagation constant and the time dependence $e^{j\omega t}$ has been suppressed.

2.3.2 Application of The Boundary Conditions

The above equations must be evaluated subject to the appropriate boundary conditions. These are :

$E_{zI} = 0$	at	$r = c$	(2.3.8)
$E_{zII} = 0$	at	$r = b$	(2.3.9)
$E_{zII} = 0$	at	$r = c$	(2.3.10)
$E_{rII} = 0$	at	$z = L$	(2.3.11)
$E_{zIII} = 0$	at	$r = a$	(2.3.12)
$E_{rIII} = 0$	at	$z = L$	(2.3.13)

Using (2.3.8), if k_{om} denote the Zeros of $J_o(x)=o$, then the solution for the field in region I is given by

$$E_{zI} = \sum_{m=1}^{\infty} A_m J_o(k_{om} r/c) \cos(\alpha_m z) \qquad (2.3.14)$$

Application of conditions (2.3.9 - 2.3.14) to equation (2.3.4) give the field in region II as

$$E_{zII} = \sum_{n=1}^{\infty} B_n Z_o(\nu_{on} r/c) \cos\beta_n (L-z) / \cos\beta_n L \qquad (2.3.15)$$

where ν_{on} are the zeros of the transcendental equation

$$J_o(\nu) N_o(\nu/x) - J_o(\nu/x) N_o(\nu) = 0 \qquad (2.3.16)$$

and where x is given by the ratio c/b which is larger than unity. Furthermore, using conditions (2.3.12) and (2.3.13) with equation (2.3.5) results in the expression for the field in region III as

$$E_{zIII} = \sum_{p=1}^{\infty} D_p J_o(k_{op} r/a) \cos\gamma_p (L-z) / \cos\gamma_p L \qquad (2.3.17)$$

where k_{op} are the zeros of $J_o(x) = 0$.

2.3.3 Interface Matching

Continuity of the fields across the interfaces is a necessity at every point. Hence considering the interface of the regions at z = s, we match the radial and longitudinal components of the electric field and we use the orthogonality property of the Bessel functions to obtain a solution.

For the longitudinal component of the electric field we obtain

$$\int_0^a E_{zI}\, r\, J_o(k_{oq} r/a)\, dr = \int_0^a E_{zIII}\, r\, J_o(k_{oq} r/a)\, dr \qquad (2.3.18)$$

Hence substituting for E_{zI} and E_{zIII} and solving, we obtain

$$D'_q = \frac{2c^2 k_{oq}}{J_1(k_{oq})} \sum_{m=1}^{\infty} A'_m \frac{J_o(k_{om} a/c)}{c^2 k_{oq}^2 - a^2 k_{om}^2} \qquad (2.3.19)$$

where
$$A'_m = A_m \cos\alpha_m s \qquad (2.3.20)$$

$$D'_p = \frac{D_p \cos\gamma_p (L-s)}{\cos\gamma_p L} \qquad (2.3.21)$$

For regions I and II we obtain

$$\int_b^c E_{zI}\, r\, Z_o(\nu_{os} r/c)\, dr = \int_b^c E_{zII}\, r\, Z_o(\nu_{os} r/c)\, dr \qquad (2.3.22)$$

and similarly, this results in

$$B'_s = \frac{2(c/b)\nu_{os} Z_1(\nu_{os} b/c)}{(c/b)^2 Z_1^2(\nu_{os}) - Z_1^2(\nu_{os} b/c)} \sum_{m=1}^{\infty} \frac{A'_m J_o(k_{om} b/c)}{k_{om}^2 - \nu_{os}^2} \qquad (2.3.23)$$

where
$$B'_s = B_s \cos\beta_s (L-s) \,/\, \cos\beta_s L \qquad (2.3.24)$$

In order to match the radial component of the fields, we make use of the condition $E_{rI} = o$ at $z = s$, $a \leq r \leq b$. Hence the resultant equation is

$$\int_0^c E_{r1}\, r\, J_o(k_{ot} r/c)\, dr = \int_b^c E_{rII}\, r\, J_o(k_{ot} r/c)\, dr + \int_0^a E_{rIII}\, r\, J_o(k_{ot} r/c)\, d \tag{2.3.25}$$

At this stage it is convenient to introduce the following notation

$$R_{Am} = (c\alpha_m / k_{om}) \tan\alpha_m s \tag{2.3.26}$$

$$R_{Bn} = (c\beta_n / \nu_{on}) \tan\beta_n (L-s) \tag{2.3.27}$$

$$R_{Cp} = (a\gamma_p / k_{op}) \tan\gamma_p (L-s) . \tag{2.3.28}$$

On substituting and simplifying equation (2.3.25), we obtain

$$R_{At} A_t' \left[\frac{c^2}{2} J_1^2 (k_{ot}) \right] = \sum_{p=1}^{\infty} R_{Cp} D_p' \frac{a^2 c^2}{c^2 k_{op}^2 - a^2 k_{ot}^2} \left[J_o(k_{op} a/c)\, J_1(k_{ot}) \right]$$
$$+ \sum_{n=1}^{\infty} \frac{R_{Bn} B_n' b\, c}{k_{ot}^2 - \nu_{on}^2} k_{ot}\; Z_1(\nu_{on} b/c)\, J_o(k_{ot} b/c) \tag{2.3.29}$$

This equation may be further simplified since parameters $B_n' = B_s'$ and $D_p' = D_q'$. Hence eliminating these from the equation by using (2.3.25), (3.2.26) and (3.2.27), we obtain

$$R_{At} A_t' \left[\frac{c^2}{2} J_1^2 (k_{ot}) \right] = \sum_{m=1}^{\infty} \sum_{p=1}^{\infty} \frac{R_{Cp} 2a^2 c^4 k_{op}}{J_1(k_{op})} A_m' \frac{J_o(k_{om} a/c)\, J_o(k_{op} a/c)\, J_1(k_{ot})}{(c^2 k_{op}^2 - a^2 k_{om}^2)(c^2 k_{op}^2 - a^2 k_{ot}^2)}$$
$$+ \sum_{m=1}^{\infty} \sum_{n=1}^{\infty} \frac{R_{Bn} 2c^2 \nu_{on} k_{ot}}{k_{om}^2 - \nu_{on}^2} A_m' \frac{J_o(k_{om} b/c)\, J_o(k_{ot} b/c)\, Z_1^2(\nu_{on} b/c)}{(k_{ot}^2 - \nu_{on}^2)\left[(c/b)^2 Z_1^2(\nu_{on}) - Z_1^2(\nu_{on} b/c)\right]} \tag{2.3.30}$$

Hence elimination of the unknown constants will result in a single equation which can be solved for the eigenvalues of the cavity (k_p). These eigenvalues are therefore obtained from the roots of the secular determinant

$$\begin{vmatrix} (h_{11}-x_1) & h_{12} & \cdots & h_{1n} \\ h_{21} & (h_{22}-x_2) & \cdots & \cdots \\ \cdots & \cdots & \cdots & \cdots \\ h_{n1} & \cdots & \cdots & (h_{nn}-x_n) \end{vmatrix} = 0 \qquad (2.3.31)$$

where the general expressions for the elements are given by

$$h_{mt} = \sum_{p=1}^{\infty} \frac{a^3c^4\gamma_p \tan\gamma_p (L-s)\ J_o(k_{om}a/c)\ J_1(k_{ot})}{J_1(k_{op})\{c^2k_{op}^2 - a^2k_{om}^2\}\{c^2k_{op}^2 - a^2k_{ot}^2\}}$$

$$+ \sum_{n=1}^{\infty} \frac{c^3\beta_n \tan\beta_n (L-s)\ J_o(k_{om}b/c)\ J_o(k_{ot}b/c)\ Z_1^2(\nu_{on}b/c)}{(\nu_{on}^2 - k_{om}^2)(\nu_{on}^2 - k_{ot}^2)\left[(c/b)^2 Z_1^2(\nu_{on}) - Z_1^2(\nu_{on}b/c)\right]} \qquad (2.3.32)$$

$$x_t = \frac{c^3\alpha_t \tan(\alpha_t s)\ J_1^2(k_{ot})}{4k_{ot}} \qquad (2.3.33)$$

and the eigenvalues k_p are related to γ_p and β_n as shown in (2.3.6)

From the resulting eigenvalues, the resonant frequency and the field pattern can be calculated. The accuracy of the solution depends on the order of the determinant.

2.3.4. Numerical Solution of The Eigenvalues

Equation (2.3.31) was solved on an IBM 360/65 system to obtain the eigenvalues of the fifth cell in the second tank of the ING linear accelerator for the Atomic Energy of Canada, Ltd. The cavity dimensions in meters were : L = 0.1755, s = 0.058, a = 0.0125, b = 0.06 and c = 0.33. Various sizes of the determinant were used in the calculations until the change in the eigenvalue k was numerically insignificant. Theoretically the truncated size of this determinant can be estimated by evaluating the difference in h_{mt} for k and $(k + \delta k)$ iteratively until it becomes less than ε, i.e.

$$h_{mt}(k \pm \delta k) - h_{mt}(k) < \varepsilon \tag{2.3.34}$$

$$x_t(k \pm \delta k) - x_t(k) < \varepsilon \tag{2.3.35}$$

where δk is the accuracy desired in the eigenvalue and ε is smaller than the last significant figure arising in the calculations. The larger of m or t is then chosen and the resulting curves for the variation in the eigenvalue with various sizes of the determinant for the TM_{olo} and TM_{o12} modes are shown in Figs 2.3.3 and 2.3.4. The determinant was evaluated by pivotal condensation and an iterative technique was used to evaluate the eigenvalue. The computing time for a 20 x 20 determinant was approximately three minutes and due to fast convergence only 20-40 terms in the series for h_{mt} were found necessary. The resulting eigenvalues are then used to calculate the resonant frequencies which are tabulated in table 2.3.1. Table 2.3.2 shows the variation in the eigenvalues with the order of the determinant. The axial field distribution for the dominant mode in the cavity was calculated and plotted in fig 2.3.5 where it is also compared with the experimental data for the field dis-

TABLE 2.3.1.

MODE	EIGENVALUE	RESONANT FREQ.
TM_{olo}	.068	325 Mc/s
TM_{o12}	.0975	465 Mc/s
TM_{o14}	.127	607 Mc/s
TM_{o16}	.134	643 Mc/s
TM_{o18}	.145	694 Mc/s

Eigenvalues and Resonant Frequencies for Various Modes in the ING Cavity

TABLE 2.3.2

MODE	ORDER OF DETERMINANT			
	4	8	15	20
TM_{010}	.038	.068	.068	.068
TM_{012}	.067	.0818	.0955	.0975
TM_{014}	.0995	.120	.126	.127
TM_{016}	.109	.114	.132	.134
TM_{018}	.117	.139	.144	.145

Variation of Eigenvalues With Order of Determinant

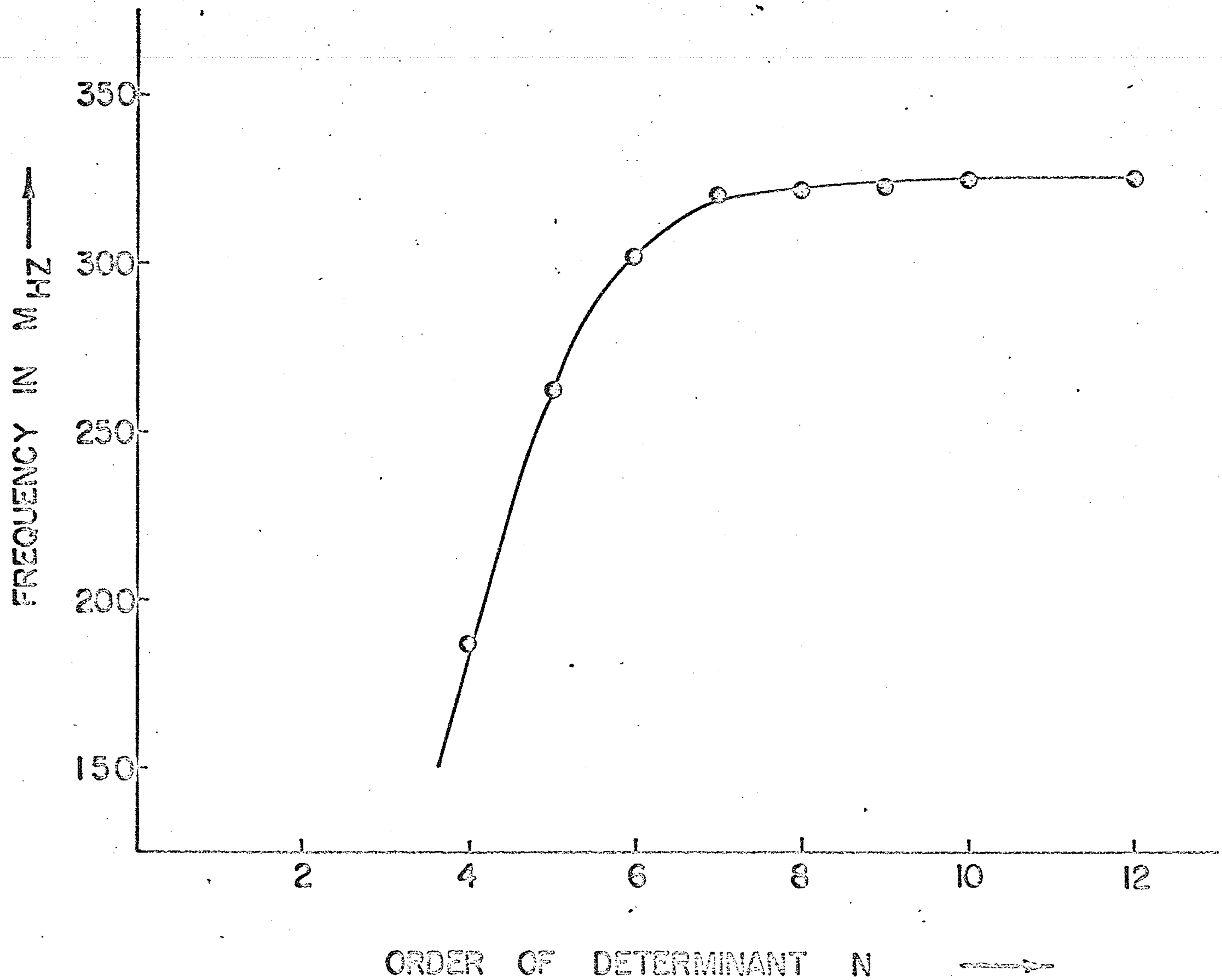

FIG. 2.3.3 RESONANT FREQUENCY FOR THE TM_{010} MODE

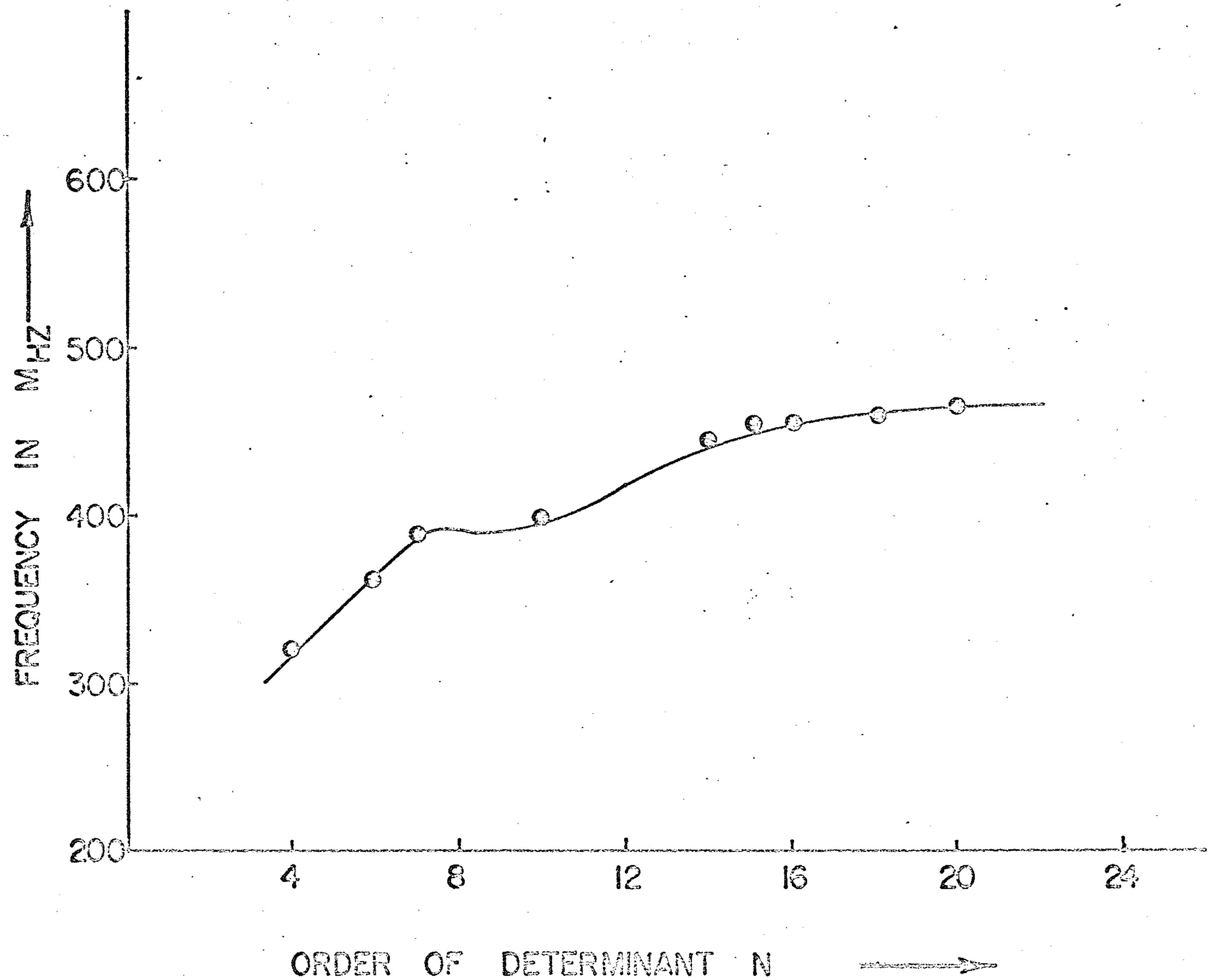

FIG.2.3.4. RESONANT FREQUENCY FOR THE TM_{012} MODE

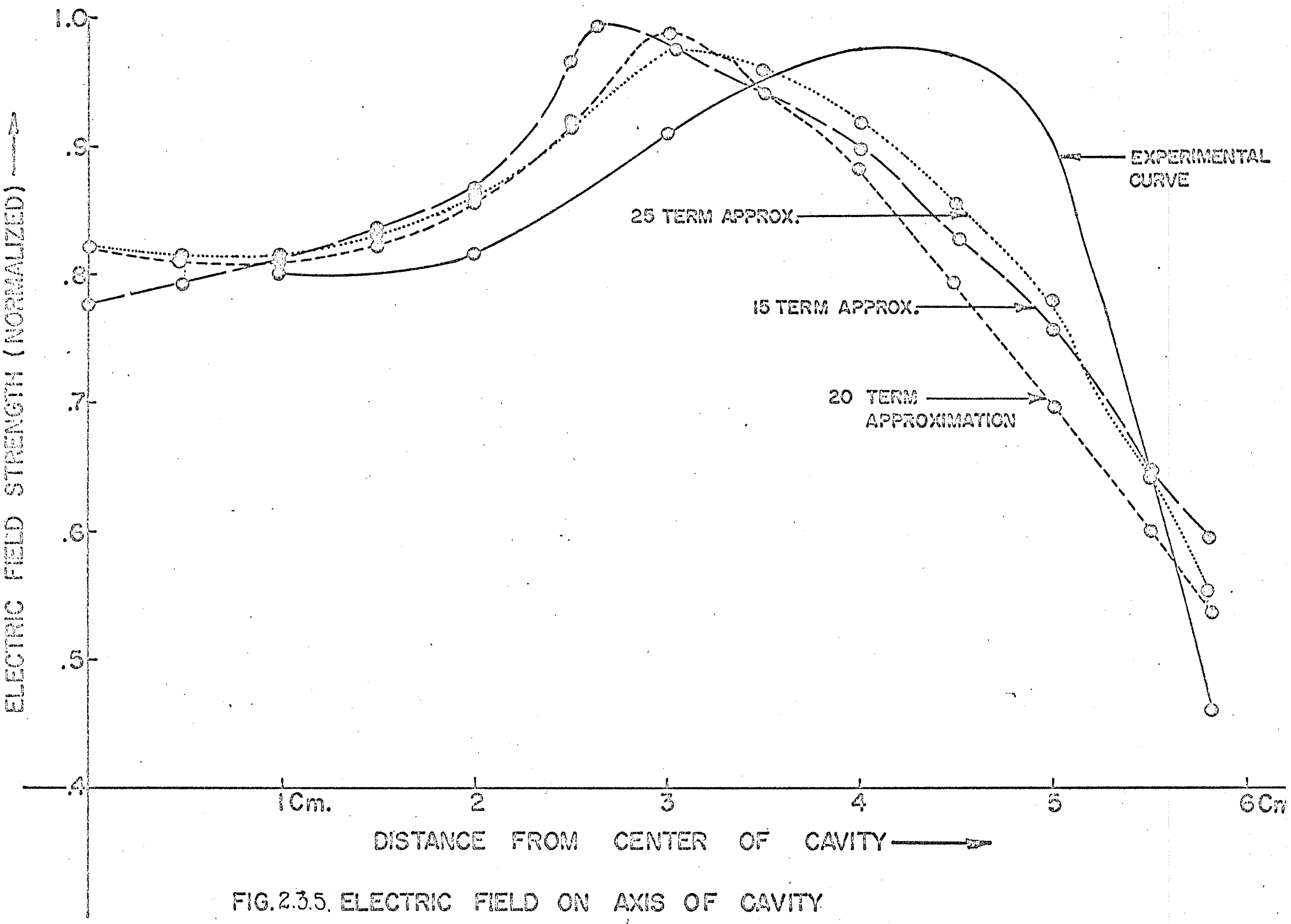

FIG. 2.3.5. ELECTRIC FIELD ON AXIS OF CAVITY

tribution in a cavity with a stem supported drift tube. The size of the drift tube is the same as above but the stem which was not accounted for in our calculations, is a cylinder 27 cm long and 3.2 cm in diameter.

2.4 Field Expressions for the TM_{olo} Mode

For the TM_{olo} mode we have

$$E_{zI} = \sum_{m=1}^{\infty} A_m J_o(k_{om} r/c) \cos(\alpha_m z) \tag{2.4.1a}$$

$$E_{zII} = \sum_{n=1}^{\infty} B_n Z_o(\nu_{on} r/c) \cos\beta_n (L-z) \;/\; \cos\beta_n L \tag{2.4.1b}$$

$$E_{zIII} = \sum_{p=1}^{\infty} D_p J_o(k_{op} r/a) \cos\gamma_p (L-z) \;/\; \cos\gamma_p L \tag{2.4.1c}$$

For each of the regions the corresponding magnetic field expressions are given by

$$H_{\theta I} = \sum_{m=1}^{\infty} \frac{i\omega Am}{Ck_{om}} J_1 \left(\frac{k_{om} r}{c}\right) \cos\alpha_m Z \tag{2.4.2a}$$

$$H_{\theta II} = \sum_{n=1}^{\infty} \frac{i\omega Bn}{C\nu_{on}} Z_1 \left(\frac{\nu_{on} r}{c}\right) \cos\beta n(L-Z)/\cos\beta nL \tag{2.4.2b}$$

$$H_{\theta III} = \sum_{p=1}^{\infty} \frac{i\omega Dp}{Ck_{op}} J_1 \left(\frac{k_{op} r}{a}\right) \cos\gamma_p (L-Z)/\cos\gamma_p (L) \tag{2.4.2c}$$

where C is the velocity of light.

Besides these the radial components of the electric field E_r exist, but are of no immeadiate interest.

2.5 Evaluation of the Q

Once the field expressions have been obtained it is a simple matter to obtain the Q of the cell. The Q is defined by the basic relation:

$$Q = \frac{\omega \text{ x time average energy stored in the system}}{\text{energy loss per second in the system}} \tag{2.5.1}$$

where ω is the circular frequency in radians/sec.

The total time average energy stored in the system is equal to the sum of the electric and magnetic energy. The time average electric and magnetic energy stored in the cavity, at resonance, are equal [15].

For the fundamental mode the magnetic field has only a θ component and the energy stored in a length L is easily evaluated by the following expression.

$$W_m = \frac{\mu_o}{4}\left[\int_0^{2\pi}\int_0^{c}\int_0^{s}(H_{\theta I}\cdot H_{\theta I}^*)\, r\, dr\, d\theta\, dz + \int_0^{2\pi}\int_b^{c}\int_s^{L}(H_{\theta II}\cdot H_{\theta II}^*) r\, dr\, d\theta\, dz\right.$$

$$\left. + \int_0^{2\pi}\int_0^{a}\int_s^{L}(H_{\theta III}\cdot H_{\theta III}^*)\, r\, dr\, d\theta\, dz\right] = W_e \tag{2.5.2}$$

where W_e is the energy stored in the electric field.

In order to evaluate W_m, we denote the integrals in (2.5.2) by I_1, I_2 and I_3, respectively, such that

$$W_m = \{\mu_o/4\}\{I_1 + I_2 + I_3\} \tag{2.5.3}$$

Using the following expressions for the magnetic field in the three regions of interest

$$H_{\theta I} = \sum_{m=1}^{\infty} \frac{A_m i k_1}{k_{om}} J_1(k_{om} r/c)\cos(\alpha_m z) \tag{2.5.4}$$

$$H_{\theta II} = \sum_{n=1}^{\infty} \frac{B_n ik_1}{\nu_{on}} Z_1(\nu_{on} r/c) \frac{\cos \beta_n (L-z)}{\cos \beta_n L} \tag{2.5.5}$$

$$H_{\theta III} = \sum_{p=1}^{\infty} \frac{D_p ik_1}{k_{op}} J_1(k_{op} r/a) \frac{\cos \gamma_p (L-z)}{\cos \gamma_p L} \tag{2.5.6}$$

and the orthogonality conditions of the Bessel functions, we obtain

$$I_1 = \sum_{m=1}^{\infty} \frac{A_m^2 k_1^2 \pi c^2}{2k_{om}^2} J_1^2(k_{om})[s + 0.5\sin(2\alpha_m s)]\sum_{t=1}^{\infty} \frac{\cos\alpha_m s \ \sin\alpha_t s}{\alpha_m - \alpha_t}, \quad m \neq t \tag{2.5.7}$$

$$I_2 = \sum_{n=1}^{\infty} \frac{B_n^2 k_1^2 \pi}{\nu_{on}^2 \cos^2\beta_n L} [(L-s)-0.5\sin 2\beta_n (L-s)]\sum_{u=1}^{\infty} \frac{\cos\beta_n (L-s)\sin\beta_u (L-s)}{\beta_n - \beta_u} \Big[0.5c^2 [$$

$$J_1^2(\nu_{on}) - J_0(\nu_{on})J_2(\nu_{on})] - 0.5b^2 [J_1^2(\nu_{on} b/c) - J_0(\nu_{on} b/c) J_2(\nu_{on} b/c)]$$

$$- 0.5c^2 \frac{J_0(\nu_{on})}{N_0(\nu_{on})} [J_1(\nu_{on})N_1(\nu_{on}) + J_0(\nu_{on})N_2(\nu_{on}) + J_2(\nu_{on})N_0(\nu_{on})]$$

$$- \frac{0.5b^2}{N_0(\nu_{on})} [J_1(\nu_{on} b/c)N_1(\nu_{on} b/c)J_0(\nu_{on}) - J_0(\nu_{on} b/c)N_2(\nu_{on} b/c) -$$

$$J_2(\nu_{on} b/c)N_0(\nu_{on} b/c)J_0(\nu_{on})] + \left[\frac{J_0(\nu_{on})}{N_0(\nu_{on})} \right]^2 \{ 0.5c^2 [N_1^2(\nu_{on}) - N_0(\nu_{on})N_2(\nu_{on})]$$

$$-0.5b^2 [N_1^2(\nu_{on} b/c) - N_0(\nu_{on} b/c)N_2(\nu_{on} b/c)]\} \Big] \quad , u \neq n \tag{2.5.8}$$

$$I_3 = \sum_{p=1}^{\infty} \frac{D_p^2 k_1^2 a^2 \pi}{2k_{op}^2 \cos^2\gamma_p L} J_1^2(k_{op})[(L-s) - 0.5\sin 2\gamma_p (L-s)]\sum_{v=1}^{\infty} \frac{\cos\gamma_p (L-s)\sin\gamma_p (L-s)}{\gamma_p - \gamma_v},$$

$$v \neq p \tag{2.5.9}$$

It remains to calculate the energy lost in the system per second. The field expressions being known, this is obtained from the surface currents given by the value of H_θ at the metallic surfaces, ie.

$$P_\ell = \frac{R_m}{2}\left[\int_0^s\int_0^{2\pi} H^2_{\theta I}(z,c)\, d\theta\, dz + \int_0^{2\pi}\int_s^L H^2_{\theta III}(z,a)\, d\theta\, dz + \int_0^{2\pi}\int_s^L H^2_{\theta II}(z,b)\, d\theta\, dz + \int_0^{2\pi}\int_s^L H^2_{\theta II}(z,c)\, d\theta\, dz + \int_0^{2\pi}\int_0^b rH^2_{\theta I}(s,r)\, dr\, d\theta + \int_0^{2\pi}\int_b^c rH^2_{\theta II}(L,r)\, dr\, d\theta\right] \tag{2.5.10}$$

where

$$R_m = \left(\frac{\omega\mu}{2\sigma}\right)^{\frac{1}{2}} \tag{2.5.11}$$

Similarly, denoting the integrals in (2.5.10) by I_4 to I_9, respectively, and we use (2.5.4) to (2.5.6) to obtain

$$P_\ell = 0.5R_m\ [\ I_4+I_5+I_6+I_7+I_8+I_9\ ] \tag{2.5.12}$$

where

$$I_4 = \sum_{m=1}^{\infty} \frac{A_m^2 k_1^2 \pi}{k_{om}^2} J_1^2(k_{om})[s + 0.5\sin 2\alpha_m s]\sum_{t=1}^{\infty}\frac{\cos\alpha_m s\ \sin\alpha_t s}{\alpha_m-\alpha_t}\ ,\quad t \neq s \tag{2.5.13}$$

$$I_5 = \sum_{p=1}^{\infty} \frac{D_p^2 k_1^2 \pi}{k_{op}^2\cos^2\gamma_p L} J_1^2(k_{op})\ [(L-s) - 0.5\sin 2\gamma_p(L-s)]\sum_{v=1}^{\infty}\frac{\cos\gamma_p(L-s)\sin\gamma_p(L-s)}{\gamma_p-\gamma_v}\ ,\quad v \neq p \tag{2.5.14}$$

$$I_6 = \sum_{n=1}^{\infty} \frac{B_n^2 k_1^2 \pi}{\nu_{on}^2\cos^2\beta_n L}\left[\ J_1(\nu_{on}b/c) - \frac{J_0(\nu_{on})N_1(\nu_{on}b/c)}{N_0(\nu_{on})}\ \right]^2 [(L-s) - 0.5\sin 2\beta_n(L-s)]$$

$$\cdot\sum_{u=1}^{\infty}\frac{\cos\beta_n(L-s)\sin\beta_n(L-s)}{\beta_n-\beta_u}\qquad u \neq n \tag{2.5.15}$$

$$I_7 = \sum_{n=1}^{\infty} \frac{B_n^2 k_1^2 \pi}{\nu_{on}^2 \cos^2\beta_n L} \left[J_1(\nu_{on}) - \frac{J_0(\nu_{on})N_1(\nu_{on})}{N_0(\nu_{on})} \right]^2 \left[(L-s) - 0.5\sin 2\beta_n (L-s) \right]$$

$$\cdot\sum_{u=1}^{\infty} \frac{\cos\beta_n(L-s)\sin\beta_n(L-s)}{\beta_n - \beta_u} \qquad u \neq n \qquad (2.5.16)$$

$$I_8 = \sum_{m=1}^{\infty} \frac{A_m^2 k_1^2 \pi}{k_{om}^2} \cos^2(\alpha_m s) \Big[b^2\{J_1^2(k_{om}b/c) - J_0(k_{om}b/c)J_2(k_{om}b/c)\} - a^2\{J_1^2(k_{om}a/c) -$$

$$J_0(k_{om}a/c)J_2(k_{om}a/c)\}\Big] \qquad (2.5.17)$$

$$I_9 = \sum_{n=1}^{\infty} \frac{2B_n^2 k_1^2 \pi}{\nu_{on}^2 \cos^2\beta_n L} \Big[0.5c^2\{J_1^2(\nu_{on}) - J_0(\nu_{on})J_2(\nu_{on})\} - 0.5b^2\{J_1^2(\nu_{on}b/c) -$$

$$J_0(\nu_{on}b/c)J_2(\nu_{on}b/c)\} - 0.5\,\frac{J_0(\nu_{on})}{N_0(\nu_{on})}\{c^2[J_1(\nu_{on})N_1(\nu_{on}) + J_0(\nu_{on})N_2(\nu_{on}) +$$

$$N_0(\nu_{on})J_2(\nu_{on})] - b^2[J_1(\nu_{on}b/c)N_1(\nu_{on}b/c) - J_0(\nu_{on}b/c)N_2(\nu_{on}b/c) -$$

$$J_2(\nu_{on}b/c)N_0(\nu_{on}b/c)]\} + 0.5\left\{\frac{J_0(\nu_{on})}{N_0(\nu_{on})}\right\}^2\{c^2[N_1^2(\nu_{on}) - N_0(\nu_{on})N_2(\nu_{on})] -$$

$$b^2[N_1^2(\nu_{on}b/c) - N_0(\nu_{on}b/c)N_2(\nu_{on}b/c)]\}\Big] \qquad (2.5.18)$$

Hence the Q of the cavity is given by

$$Q = 2\omega W_m / P_\ell \qquad (2.5.19)$$

The Q was evaluated for the fifth cell in the second tank of the ING accelerator mentioned previously and found to be 19,183 which compares favourably with the 13,250 figure found by experiment.

2.6 Error Analysis

In actual computations, two major sources of errors occur. The first occuring in the truncation of the infinite series for h_{mt}, the elements of the determinant, and the second is in limiting the order of the determinant. Besides these, the number of significant figures to be carried in the calculation for the eigenvalues is also significant.

Consider first the error introduced in truncating the infinite series involved in computing the h_{mt} terms. For this the asymptotic behaviour of the terms for large p and n is required and the following expansions are useful. The zeros of $J_o(x)$ as x becomes large approach the zeros of $\mathrm{Cos}(x-\pi/4)$, and the zeros of $N_o(x)$ approach the zeros of $\mathrm{Sin}(x-\pi/4)$, hence the zeros of

$$J_o(\nu)\, N_o(\nu/x) - J_o(\nu/x)\, N_o(\nu) = 0$$

approach the zeros of

$$\tan(\nu/x) - \tan(\nu)$$

for ν sufficiently large and $x > 1$. This leads to

$$k_{om} \simeq (2m+1)\pi/2 + \pi/4, \quad m = 0,1,2 \ldots. \tag{2.6.1}$$

and

$$\nu_{on} = n\, x\, \pi/(x - 1) \quad n = 0,1,2 \ldots.. \tag{2.6.2}$$

for large m and n. Furthermore

$$Z_1^{\,2}(\nu_{on}/x)/[x^2 Z_1^{\,2}(\nu_{on}-Z_1^{\,2}(\nu_{on}/x)] = \left[[xZ_1(\nu_{on})/Z_1(\nu_{on}/x)]^2 - 1\right]^{-1}$$

$$\simeq (x-1)^{-1} \tag{2.6.3}$$

and the exact and limiting values of this function for a particular x can be compared for n sufficiently large.

To investigate the behaviour of h_{mt} we choose $p=p_o$ and $n = n_o$ sufficiently large, such that the asymptotic expansions of the Bessel function are valid.

In this instance we drop the common c^3 in (2.3.32) and (2.3.33) to obtain

$$h_{mt} = \sum_{p=1}^{p_o-1} \ldots\ldots + \sum_{n-1}^{n_o-1} \ldots\ldots + \sum_{p_o}^{\infty} \ldots\ldots + \sum_{n_o}^{\infty} \ldots\ldots \tag{2.6.4}$$

where the last two terms represent the error occuring in the truncation.

For the particular values $p=p_1$, $n=n_1$, such that $p_1>p_o$ and $n_1>n_o$, and sufficiently large to ensure that,

$$k_{op}^2,\ \nu_{on}^2 \gg k_{om}^2,\ k_{ot}^2$$

and

$$(\nu_{on}/c)^2 \gg k_o^2$$

then

$$\beta_{n_1} \tan \beta_{n_1} (L-s) \simeq x n_1 \pi / c(x-1) \tag{2.6.5}$$

and

$$\gamma_{p_1} \tan \gamma_{p_1} (L-s) \simeq [(2p_1+1)\pi/2 + \pi/4]/a \tag{2.6.6}$$

Thus the error term is given from (2.6.4) by

$$E_{mt} = \sum_{p_o}^{\infty} \ldots\ldots\ldots + \sum_{n_o}^{\infty} \ldots\ldots\ldots$$

$$= \sum_{p=p_o}^{\infty} \frac{a^3 c\ \gamma_p \tan\gamma_p (L-s)\ J_o(k_{om} a/c)\ J_1(k_{ot})}{J_1(k_{op})\{c^2 k_{op}^2 - a^2 k_{om}^2\}\{c^2 k_{op}^2 - a^2 k_{ot}^2\}}$$

$$+ \sum_{n=n_o}^{\infty} \frac{\beta_n \tan\beta_n (L-s) J_o(k_{om} b/c) J_o(k_{ot} b/c)}{(x-1)\ (\nu_{on}^2 - k_{om}^2)(\nu_{on}^2 - k_{ot}^2)} \tag{2.6.7}$$

Upon substitution of (2.6.5) and (2.6.6) with the limiting assumptions

$k_{op}^2 >> k_{om}^2$ or k_{ot}^2, and simplifying, we obtain

$$E_{mt} = a/c^3 (a/2c)^{\frac{1}{2}} J_o(k_{om} a/c) J_1(k_{ot}) \sum_{p=p_o}^{\infty} \frac{c+[(2p+1)\pi/2-\pi/4]a}{[(2p+1)\pi/2-\pi/4]^3}$$

$$+ \frac{x-1}{cx^2\pi^2} J_o(k_{ot} b/c) J_o(k_{om} b/c) \sum_{n=n_o}^{\infty} 1/n^2 \qquad (2.6.8)$$

Simplifying further with $\pi p >> \pi/4$ we have

$$E_{mt} = a/c^3 (a/2c)^{\frac{1}{2}} J_o(k_{om} a/c) J_1(k_{ot}) \sum_{p=p_o}^{\infty} (c+\pi p)/\pi^3 p^3$$

$$+ \frac{x-1}{cx^2\pi^2} J_o(k_{ot} b/c) J_o(k_{om} b/c) \sum_{n=n_o}^{\infty} 1/n^2 \qquad (2.6.9)$$

Thus it follows, that for a higher degree of accuracy, we could compute the h_{mt} terms by first using the equation (2.3.32) to a certain degree say p,n equal 20 or 40 each and then use (2.6.9) to correct these.Thus considerable computational time is saved due to the asymptotic approximation, and a high degree of accuracy is maintained. The order of the secular determinant which is another source of error, must now be considered. As $(L-s) \to 0$, $h_{mt} \to 0$ and in the limit $(L-s)=0$, only the diagonal terms of the determinant remain and the successive eigenvalues (k_o) are obtained from the successive terms in the diagonal. Hence it may be concluded that the eigenvalues of the perturbed cavity are associated with the corresponding diagonal terms and are perturbed from their value for L-s=0 by the off diagonal terms.

For the lowest eigenvalues of interest, $\alpha_t, \beta_n, \gamma_p$ are sufficiently large for large t,n and p and become independent of k_o since

$$k_o >> k_{ot}/c \text{ or } \nu_{on}/c \text{ or } k_{op}/a$$

As m and $t \to \infty$, $h_{mt} \to 0$ and similarly we can show that $x_t \to 0$. Hence h_{mt} and x_t are not only insensitive to changes in k_o, as m and t increase, but also tend to zero.

Since the behaviour of $\Delta(k_o)$ as a function of k_o, alone is of interest, only that part of the determinant, sensitive to changes in k_o should be considered. This allows us to determine the size of the determinant by inspecting the sensitivity of the coefficients to a change in k_o. Thus if $\delta\, k_o$ is the accuracy desired in k_o, then the largest m and t are chosen such that

$$h_{mt}(k \pm \delta k_o) - h_{mt}(k) < \varepsilon \tag{2.6.10}$$

and

$$x_t(k \pm \delta k_o) - x_t(k) < \varepsilon \tag{2.6.11}$$

The larger of m and t determines the order of the determinant to be used in the calculations.

CHAPTER III

EVALUATION OF IMPORTANT LINAC PARAMATERS

The work of the last chapter can be used further to develop expressions for some basic linac paramaters which are of importance in measuring performance and in the choice of competing cavity designs. In this chapter the expressions are obtained for the transit time factor and the shunt impedance for the Alvarez structure taking into account the effects of the beam guiding hole.

3.1 Basic Energy Relations, Transit Time and Impedance Concepts

Consider the simple but practical accelerator consisting of right circular cylindrical cells as shown in Figure 3.1.1. With excitation at the correct frequency each cell resonates in the TM_{olo} mode. The electric field has only a z component with no z dependence and a maximum value on the axis, while the magnetic field has a θ component which is zero on the axis. The holes in the wall are assumed not to disturb the field and the expressions for E_z and H_θ may be written as follows [16]:

$$E_z = \frac{k^2}{j\omega\varepsilon} J_o\left(\frac{x_{o1} r}{a}\right) \tag{3.1.1}$$

$$H_\theta = \frac{x_{o1}}{a} J_1\left(\frac{x_{o1} r}{a}\right) \tag{3.1.2}$$

The peak voltage across the cell is

$$\Delta V_o = \int_{-L/2}^{L/2} E_o dz = E_o L \tag{3.1.3}$$

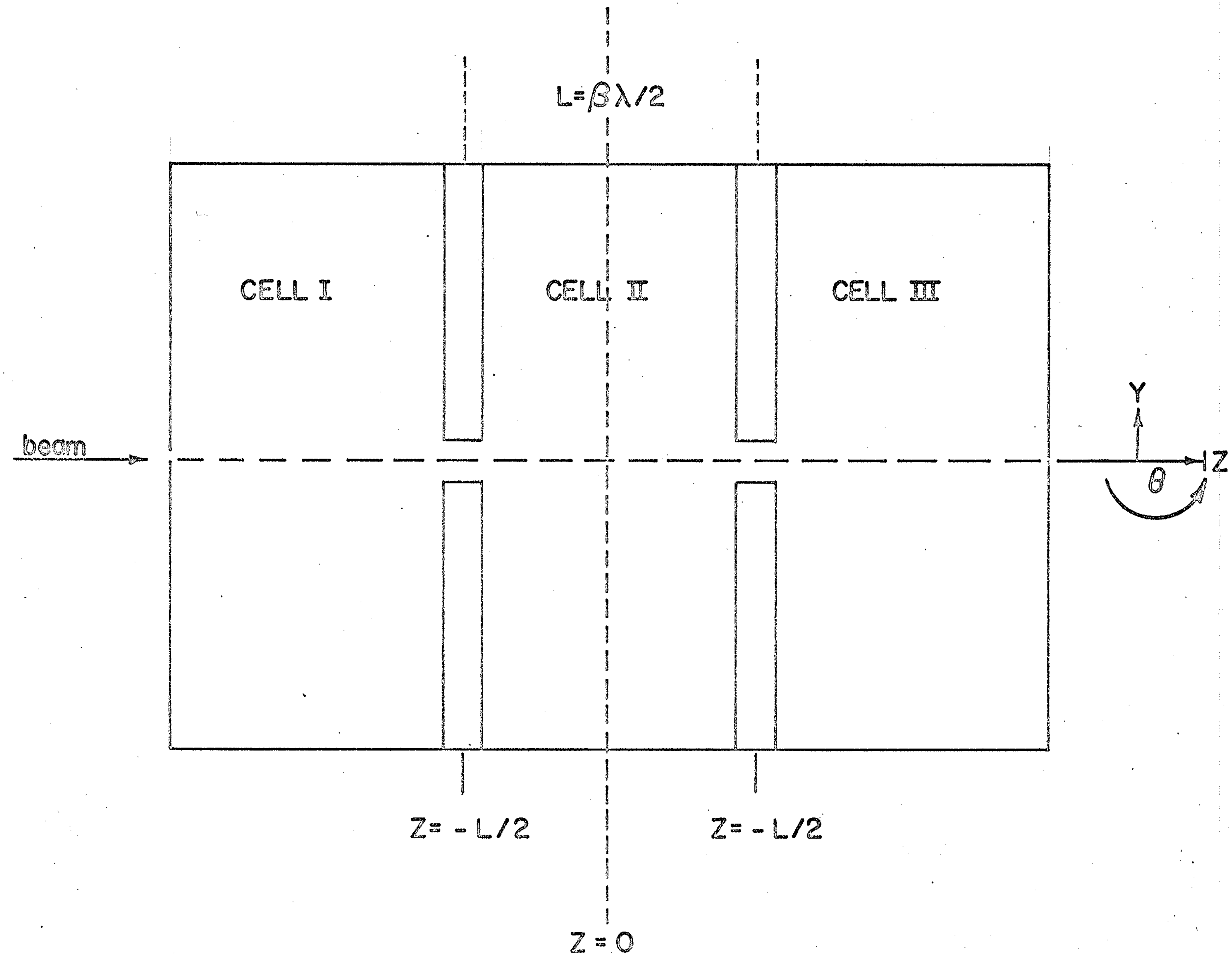

FIG. 3.1.1 A SIMPLE ACCELERATING STRUCTURE

and a particle crossing the cell at the instant of peak voltage gains an energy

$$\Delta W_o = eE_oL \tag{3.1.4}$$

But finite time is required for traversing the length of the cell and if the particle passes the centre of the cell when the electric field is maximum and ϕ is the phase of the particle with respect to the r.f. field at the centre of the cell, the actual energy gain for a relativistic particle is [17]

$$\Delta W_s = e\int_{-L/2}^{L/2} E_o \mathrm{Cos}(\pi z/L)dz \tag{3.1.5}$$

The ratio $\frac{\Delta Ws}{\Delta Wo}$ is called the <u>longitidunal transit time factor</u> (T_1) and is always less than 1. So the energy gain is

$$\Delta W_s = eE_oT_1L \tag{3.1.6}$$

If E_o is increased to E_o' and the particle made to pass the centre at a phase ϕ_s the same energy gain can be obtained

$$\Delta W_s = eE_o'T_1L\mathrm{Cos}\phi_s \tag{3.1.7}$$

The energy of the particle will depend on its phase. For a proton this results in an incorrect average velocity and a shift of phase of the particle with respect to the r.f. wave. A particle arriving too early at the centre gains energy less than ΔW_s and so slips back. A late particle gains more energy and hence catches up to ϕ_s. Particles with $\phi = \phi_s$ are called synchronous particles.

Thus there is a certain stability range in ϕ_s about which there is a restoring force tending to bunch the particles about ϕ_s. The existence of phase stability requires that the beam be unstable to radial motion so that auxilliary focussing is necessary to confine the beam along the axis of the accelerator.

The r.f. power required to establish the field E'_o in a cell is given as

$$P = \frac{(E'_o L)^2}{ZL} \tag{3.1.8}$$

where Z = normal shunt impedance of the cell and for convenience the effective shunt impedance is defined:

$$P = (E'_o TL)^2 / R_s L \tag{3.1.9}$$

where

$$R_s = ZT^2 \tag{3.1.10}$$

The complete transit time factor T is much more complex and is the one used for computational purposes. This includes the effects of spatial distribution of electric fields, its time variation and the radial field variation taking into account the holes for beam guidance. The transit time factor is improved by adding drift tubes.

3.2. The Transit Time Factor For The Linac Cavity, Considering the Beam Guiding Hole

The transit time factor has been investigated for a linac cavity by Gluckstern [14] but this has its limitations in so far as the effects of the beam guiding hole were neglected. Using the definition given above for the transit time factor, and the work of Gluckstern, we can arrive at an expression for evaluating the above factor, considering the effects of the drift tube bore.

The energy gain of a particle of charge 'q' in passing through a length 2L of the cavity under consideration is given by

$$\delta E = q \left[\int_0^S E'_{zI}(z,0) \cos \frac{\omega z}{v} \, dz + \int_S^L E'_{zIII}(z,0) \cos \frac{\omega (L-z)}{v} \, dz \right] \tag{3.2.1}$$

where the primed notation indicates that the field is evaluated at a particular radius, and v is the velocity of the particles.

Moreover, the ideal energy gain for a particle is given by

$$E_q = q \left[\int_0^S E'_{zI}(z,0) \, dz + \int_S^L E'_{zIII}(z,0) \, dz \right] \tag{3.2.2}$$

Hence the transit time factor 'T ' is given by

$$T = \delta E / E_q \tag{3.2.3}$$

3.3 The Shunt Impedance Of The Structure

For judging the relative merit of competing cavity designs, a high energy gain of the particles in passing through the cavity per unit of power loss is required. ZT^2, the effective shunt impedance,is related to energy gain and power loss by equation (3.3.1) and is hence a useful paramater for judging such performance.

$$ZT^2 = \frac{1}{q^2 L} \left[\frac{(\delta E)^2}{P_\ell} \right] \tag{3.3.1}$$

where δE = energy gain of the particles in passing through the cavity.

P_ℓ = Power loss in the cavity .

Amongst other things, the Q of the cavity, transit time factor and maximum electric field at the metallic surface are also used, but ZT^2

remains as the principal measure of performance.

Having found expressions for the losses and the energy gain of a particle of charge q in passing through the structure we can proceed to obtain an expression for the shunt impedance.

The effective shunt impedance per unit length may be defined as

$$R_s = (\Delta W)^2/P_1 L \qquad (3.3.2)$$

where ΔW is the maximum energy gain for a particle of synchronous energy, including the Transit Time Factor and effects of the drift tube bore, while P_1 is the loss in the system for the same length L as given by equation (2.3.10) and ΔW is given by the relation

$$\Delta W = q \left[\int_0^S E'_{zI}(z,0) \cos \frac{\omega z}{v}\, dz + \int_S^L E'_{zIII}(z,0) \cos \frac{\omega(L-z)}{v}\, dz \right] \qquad (3.3.3)$$

Hence evaluation of ΔW and P_1 for a particular geometry will lead to the shunt impedance through equation (3.3.2).

The shunt impedance for a drift tube supported by a stem has been calculated by Trubetskoj [18] as that for a coaxial line having an internal diameter equal to the diameter of the supporting tube (d) and an external diameter $D = \beta\lambda/2$, where λ is the wave length in vacuum. He obtains an expression of the form

$$R_s = \frac{250}{\lambda^{\frac{1}{2}}} \frac{d}{D} \ln^2 \frac{D}{d} \frac{\mathrm{Sin}^2 ml}{ml + .5\mathrm{Sin}2ml} \quad \mathrm{M}\Omega/\mathrm{m} \qquad (3.3.4)$$

where l is the length of the supporting tube as shown in figure 3.3.1.

The value $ml = 2\pi l/\lambda$ is dependent on β, as well as on the diameter of the drift tube, and on the ratio α of the accelerating gap length to D.

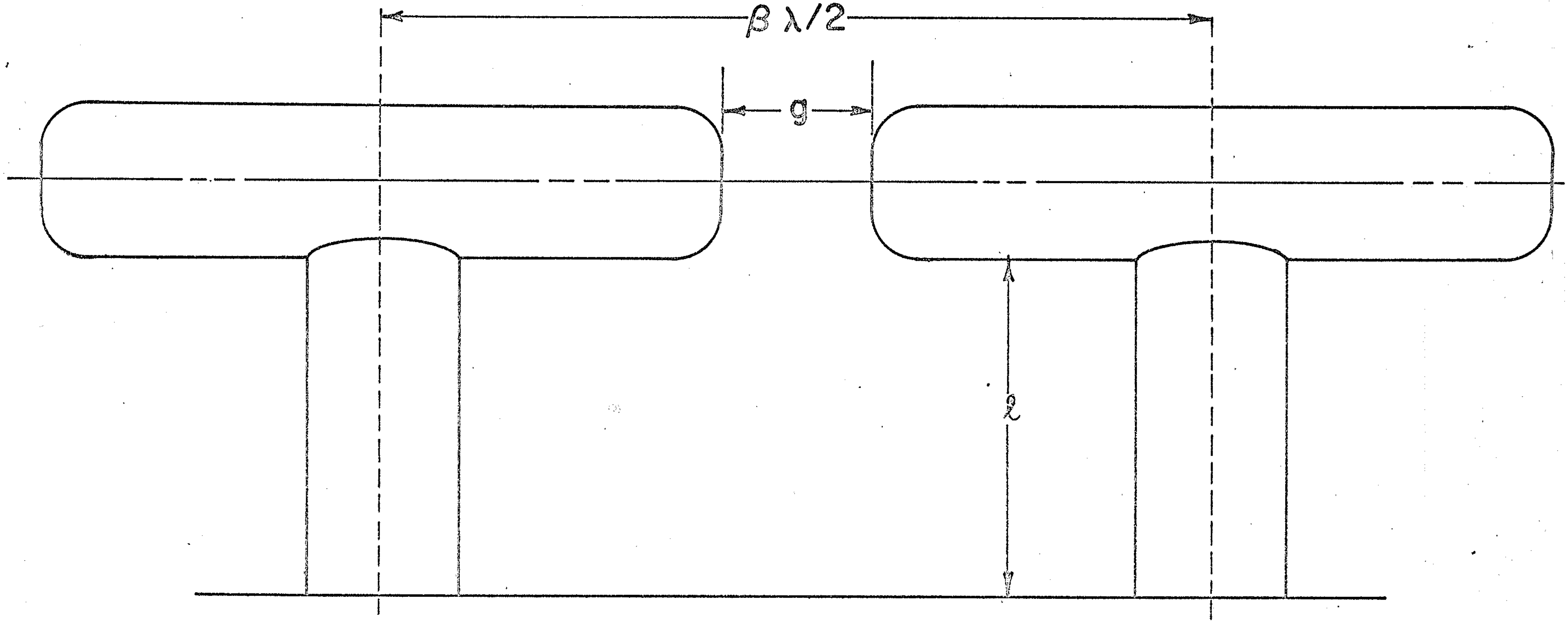

AN ACCELERATING SYSTEM CAPABLE OF WORKING WITHIN WIDE ENERGY LIMITS OF ACCELERATING PARTICLES.

FIG. 3.3.1.

Finally the ratio of peak to average field gradient defined by

$$E_{max}/E_{av}=E_{max}.L/\left(\int_{0}^{s} E'_{zI}(z,o)dz + \int_{s}^{L} E'_{zIII}(z,o)dz\right) \qquad (3.3.5)$$

may be evaluated, which is an important factor in considering the maximum field allowed before sparking takes place.

3.4 Results For The ING Cavity

The transit time factor and the effective shunt impedance were calculated for the experimental cavity of the last chapter for various values of 'β', the relativistic velocity factor. Table 3.4.1 shows the values obtained. Due to inadequacy of the experimental setup, no experimental checks were possible.

TABLE 3.4.1

β	Transit Time Factor	Shunt Impedance in MΩ/m
0.25	0.9394	54.36
0.30	0.8944	49.28
0.35	0.8620	45.78
0.40	0.8387	43.34
0.45	0.8218	41.60
0.50	0.7091	40.33
0.55	0.7994	39.37
0.60	0.7919	38.63
0.65	0.7860	38.05
0.70	0.7812	37.59
0.75	0.7773	37.22
0.80	0.7741	36.91
0.85	0.7714	36.66
0.90	0.7691	36.44
0.95	0.7672	36.26

Transit Time Factor and Shunt Impedance Vs 'β'

CHAPTER IV

DISCUSSION AND CONCLUSIONS

4.1 Discussion of The Results

Examination of our results shows that it is not necessary to use a very high order determinant in evaluating the first eigenvalue, due to the rapid convergence. However, for the higher order modes, a large determinant is required before convergence occurs. The poor agreement between the experimental and theoretical results for the eigenvalue arises from the fact that the experimental cavity shown in Figure 4.1.1 had a stem designed to support the drift tube. This naturally lowers the resonant frequency and hence the eigenvalue. The resonant frequencies evaluated for the higher order modes are likely to be in error as these are given on the basis of a 20 x 20 determinant which may not be adequate for higher order mode evaluation.

The plot in Figure 2.3.5 for E_z is seen to agree quite well with that obtained by measurements based on perturbation techniques. The measurement method is not very accurate for fields near the plates and since the accelerating gap is quite small, no high degree of accuracy can be expected in the measured values. The theoretical prediction for the field is seen to resemble that obtained by Hoyt [11]. A high degree of accuracy is possible, however, if a large number of terms are used in the computation of the fields but this requires excessive computation time. The fields near the ends of the drift tube require a much larger number of terms and addition of effects due to the generation of higher order modes at the discontinuity which we have not accounted for.

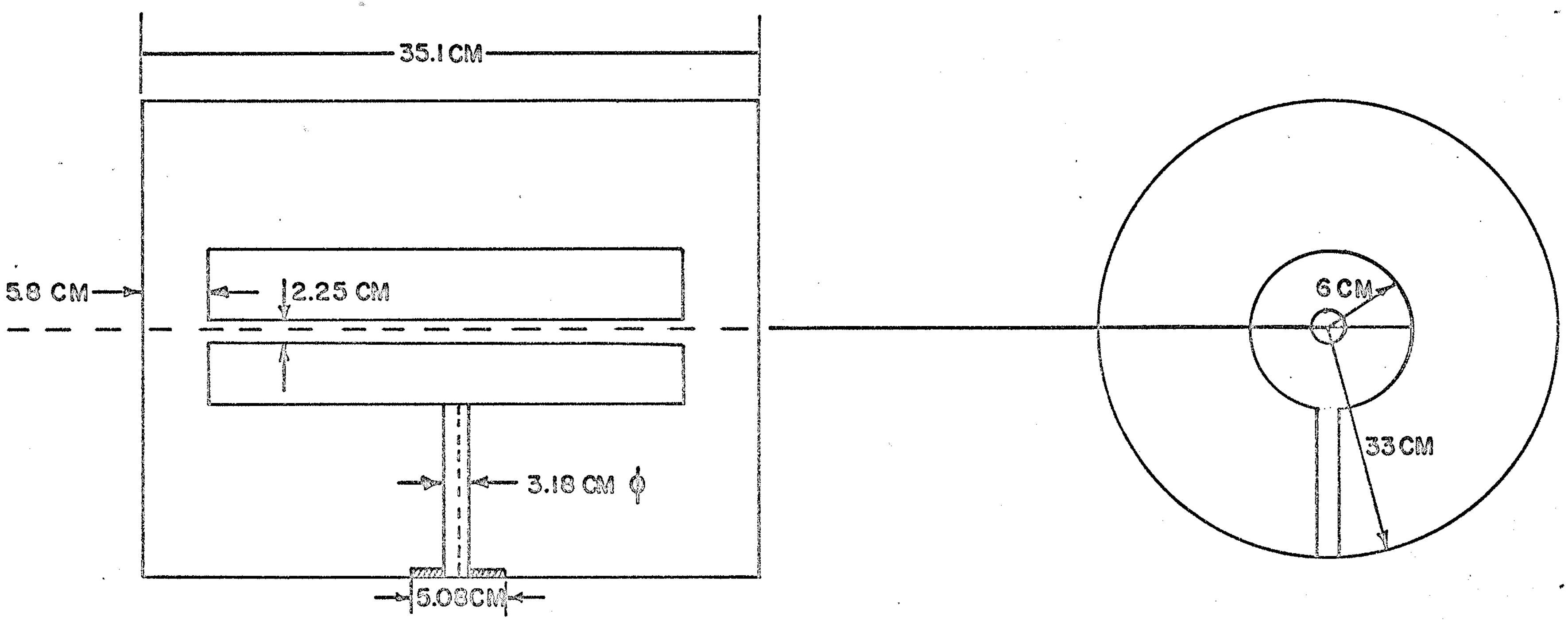

FIG. 4.1.1. THE EXPERIMENTAL CAVITY

4.2. Conclusions

In conclusion we see that this method has a wide scope in the application to problems concerning loaded structures. Although the required computations are tedious, they result nevertheless in the correct eigenfrequencies and field distributions. However, the excessive computation time required in the computer programming may not justify its use in all cases. The evaluation of higher order modes requires the iterative evaluation of a large order determinant and, furthermore, a large number of terms in the series for the elements of the determinant. The equations are found to check for the case when the beam guiding hole is not taken into account as solved by Bolle and reduces his work to a particular case of our solution. The same can be said of Gluckstern's work. The method has its advantages, however, in that there is no need to generate special functions for accelerating the rate of convergence of the series. The calculations allow a check on the number of terms to be used in the expansions, the order of the determinant and also on the number of significant figures to be used in the calculations for a desired degree of accuracy.

The method is applicable to the study of optimization of cavities for accelerators, after the geometry has been reduced to a simple configuration, and presents a basis for analysis when other simpler methods cannot be found.

4.3 Suggestions for Future Research

There is unlimited scope for research in the field of inhomogeniously filled r.f. cavities. Although the effects of stems are being investigated [19-21] and though Nishikawa [6] has used the equivalent circuit approach in investigating their effect, it is felt that a field analysis would prove more rewarding in giving a better insight into the understanding of these effects.

Besides this, problems of beam dynamics are of great importance and though considerable work has been done in this area [8,9,22,23], much remains to be explained and analysed, as for instance the transient effects connected with beam switching, beam loading, etc.

Optimization studies of various types remain to be undertaken, among them the optimization of the r.f. loop and excitation methods for the cavity. As pointed out [18], the volume of useful electromagnetic field, in which acceleration takes place, is very small compared to the total volume, and, owing to the high reactive energy accumulated in the system, strong currents exist, causing high losses. Localization of the electromagnetic field in a small volume would permit a more compact and economic accelerating system.

The optimum design of the beam guiding hole is another interesting research problem. The minimum diameter of this hole is normally set by the size of the beam so that as the drift tube diameter is increased, the ratio of the hole diameter to the drift tube diameter increases. As a result, the effective radial variation of the electric field also increases, the field on the axis being substantially lower than at a radius equal to the hole radius. This results in a large radial variation of the transit time factor which strongly couples the radial and phase motion of the particles. Again it becomes necessary to incorporate radial focusing magnets within the drift tubes and the cell length becomes impractical at low energies.

For the instrumentation engineer, this field again provides a rich ground for research and design of instruments for control, monitoring, accelerator alignment, precision phase adjustment, etc., all of which are required in linear accelerators.

As particular instances, a few general problems of current interest to accelerator designers may be mentioned. Amongst these is the investigation of the effects of the radial shifting of the drift tube in a stem supported drift tube structure. The stems are required for mechanical rigidity and though these are advantageous in certain respects [20], often a situation may arise where their sole purpose would be to support the drift tubes and it becomes necessary to remove any effects the stems may have on the field system. There is reason to believe that this may be achieved by shifting the drift tube radially. Further, even without coupling the stem problem to this, the shifted drift tube structure could still be advantageous in reducing tank detuning effects and consequently is an important problem that requires looking into.

Another problem that would be highly beneficial to designers would be the derivation of an equivalent circuit for the system from the field solutions. Though work has been reported in this area, as yet no major breakthrough has been made.

As a third example one may cite a problem that has practical significance. In the solutions of linac structures, they are commonly assumed to be simple resonant cavities and the imaging technique applied in obtaining their solution. But this approach suffers from a number of disadvantages and is not practical. Firstly, in any linac structure there are a finite number of drift tubes and, secondly, they are not of equal length and are not at equally spaced intervals. Hence this is a finite periodic structure and the field solution accounting for all the above stated features is quite difficult to obtain, especially when the structures are considered pulse fed and in the presence of the particle beam.

With the construction of higher and higher energy accelerators, the physicist has uncovered a vast amount of information about the nature of elementary particles. This has always raised questions about exploring the next energy range in accelerators. But going from one energy range to another is not a simple matter, in that each type of accelerating system has its limitations and an entirely new method of acceleration, better instrumentation, more refined control and more personnel will be required.

Thus for the physicist, engineer and mathematician this field offers an almost inexhaustible source of interesting and intriguing problems.

BIBLIOGRAPHY

1. Beringer, R., and Gluckstern, R.L., "On the Normal Modes in Linac Structures, "Yale University Int. Rep. Y-9 (1964).

2. Gluckstern, R.L., "Note on the Normal Mode Treatment of Beam Cavity Interactions and the Mode Width", BNL Accelerator Dept. Int. Rep. AADD81 (1965).

3. Nishikawa, T., "A Study of Field Distributions and Beam Loading in Proton Linacs at High Energies", I.E.E.E. Transactions on Nuclear Science. NS-12 No.3 (1965)

4. Nishikawa, T., "Normal Mode Analysis of Standing Wave Linacs - Field Excitation and Beam Loading in Linac Cavities", BNL Accelerator Dept. Int. Rep. AADD87 Nov., 1965.

5. Hereward, H.J., "Some Examples of Energy Flow in the Alvarez Structure", CERN Int. Rep. MPS/DL Int. 65-1, 1965.

6. Nishikawa, T., "Equivalent Circuit and Dispersion Relations for the Multistem Drift Tube Structure", BNL Accelerator Dept. Int. Rep AADD125 Nov., 1966.

7. Beringer, R., "Shunt Resistance of Iris Loaded Waveguides on the Loose Coupling Model", BNL Accelerator Dept. Int. Rep AADD-76, 1965.

8. Gluckstern, R.L., "Transverse Beam Blow-up in Standing Wave Linacs", Minutes of the 1964 Conference on Proton Linear Accelerators, Mura-T14 (1964), P 186.

9. Nishikawa, T. "An Approach to the Study of Beam Loading for the Linear Accelerator", Minutes of the 1964 Conference on Proton Linear Accelerators, Mura 714, (1964), P214.

10. Batchelor, K., Nishikawa, T., Watz, T., "Numerical Analysis of the R.F. Field in a Drift Tube Loaded Cavity", IEEE Trans on Nuclear Science, June, 1967, P 295.

11. Hoyt, H., Simmonds, D., Rich, W., "Computer Designed 805 MHz Proton Linac Cavities," The Review of Scientific Instruments, Vol 37, No.6, June, 1966, P 755-762.

12. Hahn, W.C., "A New Method for the Calculation of Cavity Resonators", Journal of Applied Physics, Vol 12, Jan, 1941, P 62-68.

13. Bolle, D.M., "Eigenvalue For a Centerally Loaded Circular Cylindrical Cavity", I.R.E. Transactions on M.T.T., Vol.MTT-10, No-2, March, 1962, P 132.

14. Gluckstern, R.L., "Shaped Drift Tubes and Irises for Linear Accelerators", High Energy Linear Accelerators, CERN Symposium, 1961, P 129-141.

15. Collin , R., "Foundations For Microwave Engineering", McGraw Hill Book Co., N.Y., P 324.

16. Harrington, R., "Time Harmonic Electromagnetic Fields", McGraw Hill Book Co., Ltd., N.Y., P 215.

17. Livingood, J.J., " Principles of Cyclic Particle Accelerators",Van Nostrand, Princeton, N.J., 1961, P 273.

18. Trubetskoj, V.F., "New Type of High Frequency Accelerating System for Heavy Particles in Linear Accelerators", 1961 International Conference on High Energy Accelerators, CERN Symposium, P 232-234.

19. Giordano, S., "Measurements on the Multistem Drift Tube Proton Accelerators, "BNL Accelerator Dept. Int. Rep. AGSCD-11 June, 1966.

20. Giordano, S., Hannwacker, J.P., "Studies of Multistem Drift Tube Accelerator Structures". I.E.E.E. Transactions on Nuclear Science. NS-12. June, 1967, PP 290-294.

21. Giordano, S., "A New Multistem, Drift Tube, Standing Wave, Zero Mode Proton Accelerating Structure," BNL Accelerator Dept. Int. Rep. AGSCD-7, Feb., 1966.

22. Rich, M., "Beam Dynamical Calculations with Realistic Fields in a Drift Tube Linear Accelerator", I.E.E.E. Transactions on Nuclear Science, NS-12. June, 1965, PP 639-643.

23. Leiss, J.F., "Beam Loading in Linear Accelerators". I.E.E.E. Transactions on Nuclear Science, NS-12, June, 1965. PP 566-579.